Tran, Quoc; Soowski, Wojciech Tomasz; Karstunen, Minna; Korkiala-Tanttu, Leena

Modelling of fall-cone tests with strain-rate effects

Published in:
Procedia Engineering

DOI:
10.1016/j.proeng.2017.01.029

Published: 01/01/2017

Document Version
Publisher's PDF, also known as Version of record

Please cite the original version:
Tran, Q., Soowski, W. T., Karstunen, M., & Korkiala-Tanttu, L. (2017). Modelling of fall-cone tests with strain-rate effects. Procedia Engineering, 175, 293-301. https://doi.org/10.1016/j.proeng.2017.01.029

Available online at www.sciencedirect.com

ScienceDirect

Procedia Engineering 175 (2017) 293 – 301

Procedia Engineering

www.elsevier.com/locate/procedia

1st International Conference on the Material Point Method, MPM 2017

Modelling of fall-cone tests with strain-rate effects

Quoc-Anh Tran[a], Wojciech Solowski[a,]*, Minna Karstunen[b], Leena Korkiala-Tanttu[a]

[a]*Department of Civil Engineering, Aalto University, Rakentajanaukio 4 A, 02150 Espoo, Finland*
[b]*Department of Civil and Environmental Engineering, Chalmers University of Technology, SE-412 96 Gothenburg, Sweden*

Abstract

Material Point Method (MPM) is a numerical method, which is well suited for large displacement simulations. Large displacements problems are relatively common in geotechnics, including post-failure behaviour of landslides as well as a wide range of problems involving penetration into the soil body. One of those problems is the fall-cone test, commonly used to establish the undrained shear strength and the sensitivity of saturated fine grained soils.

This paper shows a Generalized Interpolation Material Point Method (GIMP) simulation replicating published free-fall cone experiment performed on a kaolin clay. In the fall-cone tests, the penetration characteristics of the cone, such as velocity and total penetration depth depend on the soil properties. Those properties are affected greatly by the strain-rate which must be accounted for in a numerical simulation. Hence, the simulations shown uses a Mohr-Coulomb / Tresca material extended with strain-rate effects.

The presented numerical simulations are compared with the published fall-cone experiment in which displacement and force were measured. The comparison indicates that Generalized Interpolation Material Point Method and Mohr-Coulomb / Tresca model extended with strain-rate effects are able to replicate the fall-cone penetration test very well.

Peer-review under responsibility of the organizing committee of the 1st International Conference on the Material Point Method

Keywords: generalized interpolation material point method; fallcone test; strain rate effects.

1. Introduction

In geotechnical engineering, dynamic penetration is a challenging problem encountered in many practical problems such as pile driving as well as laboratory and in situ soil tests.

* Corresponding author.
E-mail address: wojciech.solowski@aalto.fi

Peer-review under responsibility of the organizing committee of the 1st International Conference on the Material Point Method
doi:10.1016/j.proeng.2017.01.029

Nomenclature

a_l	reference undrained shear strength at water content of 100%
b_l	water content parameter in the power law
$f^k_{contact}$	contact force at node k of the body
f^k_{norm}	normal force in the friction contact law at node k of the body
f^k_{stick}	sticking force in the friction contact law at node k of the body
f^k_{fric}	friction force in the friction contact law at node k of the body
G_o	dynamic shear modulus
$G_{o,ref}$	reference dynamic shear modulus at reference axial strain rate
G_u	undrained shear modulus
h	penetration depth
K	cone factor
K_u	undrained bulk modulus
S_t	sensitivity
s_u	undrained shear strength
$s_{u,theo}$	undrained shear strength determined from the theoretical method
$s_{u,ref}$	reference undrained shear strength at reference shear strain rate
Q	cone weight
w	water content
α	shear modulus - strain rate parameter in the logarithm law
β	strain rate parameter in the power law
μ	undrained shear strength - strain rate parameter in the logarithm law
υ	Poisson's ratio
$\delta\gamma$	shear strain rate
$\delta\varepsilon_q$	deviatoric shear strain rate
$\delta\varepsilon_a$	axial strain rate
$\delta\gamma_{ref}$	reference shear strain rate
$\delta\varepsilon_{a,ref}$	reference axial strain rate
ξ	current accumulating shear strains
ξ_{95}	accumulating shear strains required to obtain 95% reduction of shear strength

One of the methods which may be used to solve those problems is the Arbitrary Lagrangian-Eulerian (ALE) Finite Element Method [1], [2]. However, ALE technique could incur errors in the materials with solid-fluid transition behaviour [3] and requires a frequent mesh-update to minimize the mesh-distortion. Therefore, alternative mesh-free methods such as Smooth Particle Hydro-dynamics (SPH), Material Point Method (MPM) and later Generalized Interpolation Material Point Method (GIMP) are adopted to study the large displacement problems. Compared with SPH, MPM/GIMP is more efficient at the imposition of boundary conditions. It has been validated for range of problems, such as the penetration of a strip foundation [4], modelling of pile installation in sand [5] and the cone penetration test [6]. These studies [4-6] assume that the shear strength of soils is independent of the strain-rate effects. However, the influence of the strain-rate on the undrained shear strength, and the onset of the shear band around cylindrical surfaces of penetrometer, could be considerable because of the wide ranges of strain-rate during the penetration process.

This paper shows GIMP simulations of free-fall cone tests on the kaolin clay where the effect of strain-rate on the penetration is taken into account. The numerical results concentrate on the relationship between the undrained shear strength and the penetration depth of the free-fall cone. The numerical simulations are validated with the fall-cone experimental results [7] which measured the forces on the cone as well as the displacement field of the kaolin clay.

2. Description of the fall-cone experiment

In the series of fall-cone penetration experiments [7], the vertical displacements of the cone were measured with a high speed photography camera using Particle Image Velocimetry (PIV) analysis. Additionally, the total force acting on the cone was also recorded. In this study, those free-fall cone experiment results are used to validate the numerical simulations. The experiments used the cone with 30-degree angle and self-weight of 100g. In the test, the cone penetrated into the remoulded kaolin clay and reached its maximum displacement (h=19.5mm) after slightly less than 0.1s and rebounded approximately 70μm. Figure 1 shows the experiment setup.

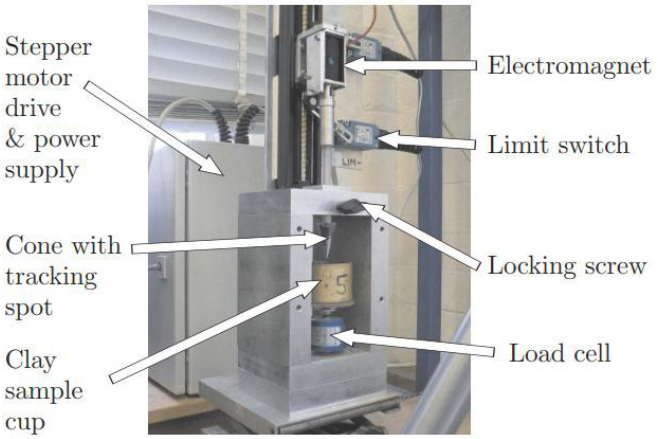

Fig. 1. Free-fall cone test experiment [7].

3. Numerical model

3.1. Description of the Generalized Interpolation Material Point Method (GIMP)

Generalized Interpolation Material Point Method (GIMP) [8] is an updated version of Material Point Method. Compared with the original formulation of MPM [9], GIMP introduced two main improvements. Firstly, GIMP introduced a particle characteristic function which helps mitigate the cell-crossing errors. In this paper, the characteristic function for the axi-symmetric GIMP interpolator described by Nairn and Guilkey [15] was used. Secondly, GIMP takes into account time-dependent particle domains which represent the current size of the material points. The presence of particle domains leads to different approaches of how the particle domains evolve in time such as uGIMP (unchanged domain volume), cpGIMP (contiguous particle domain volume without shearing deformation) [10] and CPDI (convected particle domain) [11] or CPDI2 [17]. In this paper, the approach of the uGIMP is used, as encoded in the Uintah software (http://uintah.utah.edu).

3.2. Strain rate effects

The soils sheared at different strain rates have different undrained shear strengths. Two different types of formulas can be applied to describe the influence of strain rate. For example, [12] presents the change of undrained shear strength with the shear strain $s_u(\delta\gamma)$ in logarithm cycle:

$$s_u(\delta\gamma) = s_{u,ref}(1 + \mu log\frac{\delta\gamma}{\delta\gamma_{ref}}) \quad (1)$$

where $s_{u,ref}$ is the reference shear strength at the reference strain rate ($\delta\gamma_{ref}$). The coefficient μ lies in the range of 0.1 to 0.2 for the saturated clays.

The second typical approach [12] represents the change of undrained shear strength in terms of a power law:

$$s_u(\delta\gamma) = s_{u,ref}(\frac{\delta\gamma}{\delta\gamma_{ref}})^{\beta} \quad (2)$$

with β in range of 0.05 – 0.17. Jeong [19] observed with a viscometer that both parameter μ and β are independent of the water content for low-activity clays tests.

Boukpeti et al. [13] performed number of different experiments (fall-cone tests, T-bar tests, ball penetrometer and vane shear tests) for kaolin clays and proposed a function to determine the undrained shear strength at the transition phase, taking into account the strain rate $\delta\gamma$, the water content w and the sensitivity S_t:

$$s_u(W, \delta\gamma, S_t) = a_1 w^{-b_1} (\frac{\delta\gamma}{\delta\gamma_{ref}})^{\beta} [\frac{1}{S_t} + (1 - \frac{1}{S_t}) e^{-3\xi/\xi_{95}}] \quad (3)$$

The parameters related to the influence of the water content w (a_1, b_1) are determined from (w - S_u) graph. The parameter a_1 (kPa) denotes the undrained shear strength of clays at reference water content (w = 100%) and the parameter b_1 describes the power law of the influence of the water content. These parameters can be obtained based on fall-cone tests, T-bar tests or ball tests with variation of the water contents.

The parameters related to the influence of strain rate δγ ($\delta\gamma_{ref}$, β) are determined from ($\delta\gamma$ - S_u) graph. It could be obtained approximately from the cyclic T-bar tests or ball tests with different penetration or rotation rates.

The parameters associated to the influence of sensitivity (S_t, ξ, ξ_{95}) are determined from the T-bar test and the ball test. S_t is the sensitivity of the clays and ξ, ξ_{95} are the current accumulating shear strains and accumulating shear strains required to obtain 95% reduction of shear strength. The testing procedure for determining these parameters was proposed and given by Einav [12]. The approach based on Boukpeti et al. [13] is used in the shown calculations.

3.3. Mohr-Coulomb model extended with strain rate effects

During the experiment, the fall-cone penetrated into clay under the undrained condition. Therefore, the Mohr-Coulomb soil model is used with friction angle set to zero (i.e. Tresca model). In the model, the value of cohesion represents the undrained shear strength. Figure 2 describes the schematic of the model extended with strain-rate effects. The undrained shear strength determined from equation (3) for remoulded soils is:

$$s_u(\delta\gamma) = a_1 w^{-b_1} (\frac{\delta\gamma}{\delta\gamma_{ref}})^{\beta} \quad (4)$$

The shear strain is calculated from the deviatoric strain invariant:

$$\delta\gamma = \frac{3}{2}\delta\varepsilon_q \quad (5)$$

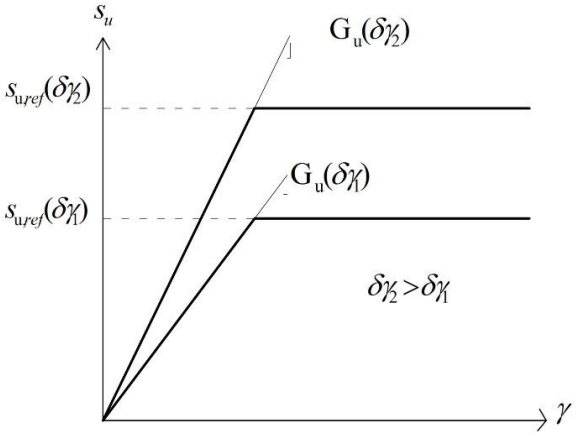

Fig. 2. Mohr-Coulomb model extended with strain-rate effect at a constant water content with strain rate with $\delta\gamma_2 > \delta\gamma_1$.

The deviatoric strain invariant is computed from the strain rate tensor as:

$$\delta\varepsilon_q = \frac{1}{3}\sqrt{2\left(\delta\varepsilon_{ii} - \delta\varepsilon_{jj}\right)^2 + 3\delta\varepsilon_{ij}{}^2} \quad (6)$$

In this study, additionally a power law is applied to represent the strain rate effect on the elastic stiffness of the soil. The undrained shear modulus (G_u) at a reference shear strain (δγ) is calculated as:

$$G_u(\delta\gamma) = G_{u,ref} (\frac{\delta\gamma}{\delta\gamma_{ref}})^{\beta} \quad (7)$$

where $G_{u,ref}$ is reference undrained shear modulus at reference strain rate ($\delta\gamma_{ref}$).

The undrained bulk modulus is calculated by a constant undrained Poisson's ratio υ=0.49.

$$K_u(\delta\gamma) = \frac{G_u(\delta\gamma) * 2(1 + \upsilon)}{3(1 - 2\upsilon)} \quad (8)$$

3.4. Friction contact between the cone-clay interface

In order to simulate the penetration of the cone into clays, it requires a contact law on the clay-cone interface. The first Coulomb friction contact for MPM was presented by Bardenhagen [14] to study the contact between granular materials. In this study, this friction contact was adopted. Figure 3 depicts the schematic of the friction contact. The Coulomb friction force is applied in the contact node "k" and along with the tangent surface which is pependicular to the normal vector n of the body. The magnitude of the friction force depends on the friction coefficient μ and the normal force f^k_{norm} computed from the projection of the contact force $f^k_{contact}$ in the normal direction as follows:

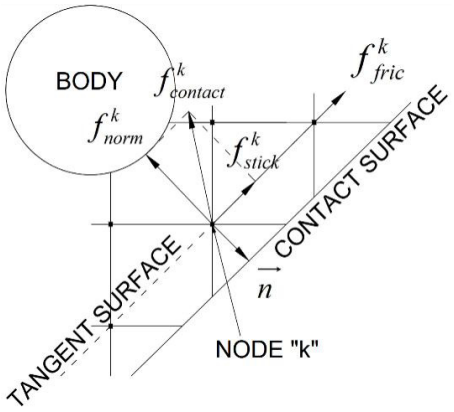

Fig. 3. Clay body – cone contact interaction.

$$f^k_{fric} = \mu * f^k_{norm} \tag{9}$$

The formulation also checks whether the contact is sliding or sticking by comparing the friction force with the sticking force f^k_{stick} computed from the projection of the contact force $f^k_{contact}$ in the tangent direction:

$$\begin{aligned} &If\ \left\|f^k_{fric}\right\| \geq \left\|f^k_{stick}\right\|\ no\ sliding \\ &If\ \left\|f^k_{fric}\right\| < \left\|f^k_{stick}\right\|\ \ sliding\ occurs \end{aligned} \tag{10}$$

3.5. Numerical model of the fall-cone test

The cone with the angle of 30 degrees and the weight of 100g was modelled using a rigid model with the axial symmetry boundary condition. Figure 4 illustrates the schematic of the numerical model. The Mohr-Coulomb with a zero friction angle and cohesion dependent on the strain rate (eq. 4) is used for the kaolin clay. The model parameters for the kaolin clay are based on the experimental results of vane shear at the reference strain rate ($\delta\gamma_{ref}$ =0.5s-1) [13] and are shown in Table 1.

Table 1. Parameters in the numerical simulation.

a_1 (kPa)	b_1	W	$\delta\gamma_{ref}$ (s^{-1})	β	$E_{u,ref}$ (kPa)	υ_u
0.205	-3.86	0.51	0.5	0.06	$500s_{u,ref}$	0.49

a_1: reference undrained shear strength at W=100% and at $\delta\gamma_{ref}$.
b_1: the inclination of the line in the (W-s_u) graph.
β: power law coefficient related to the strain rate (see eq. 4)

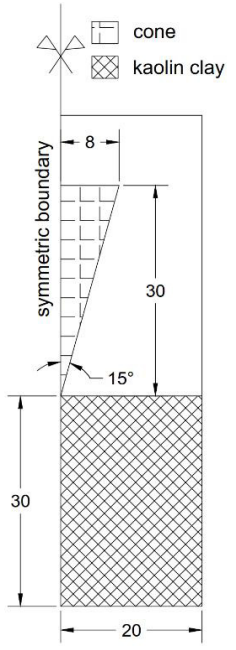

Fig. 4. Schematic of the fall-cone test. Unit in mm.

4. Study of the numerical errors

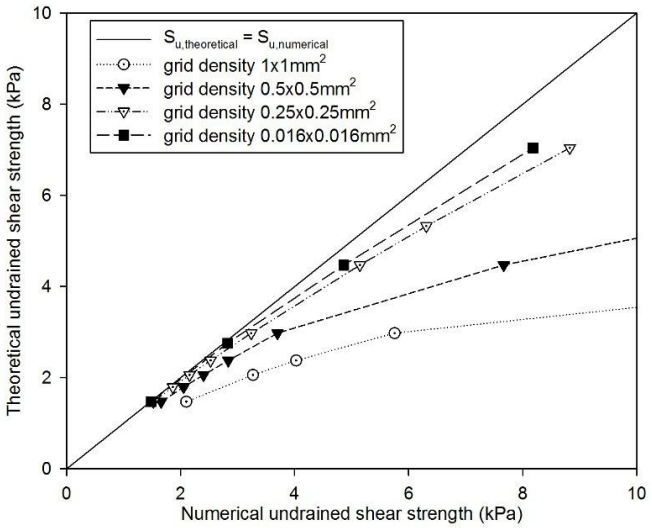

Fig. 5. Numerical errors investigation.

The accuracy of GIMP numerical simulations depends on the grid density significantly. Therefore, a series of free-fall cone simulations were carried out to investigate the grid-dependency. The numerical solutions were tested against the theoretical undrained shear strength as proposed by Koumoto & Houlsby [16]

$$s_{u,theo} = \frac{KQ}{h^2} \tag{11}$$

where Q (g) is the weight of the fall-cone; h (mm) is the penetration depth K is the fall-cone factor which depends on the type of the fall-cone, cone roughness and strain rate parameters. The cone mechanism in the experiment was assumed to be the rough cone. The rough cone with the angle of 30 degrees was used which corresponded to the cone factor K = 1.03 [16]. The friction coefficient of Coulomb contact between kaolin clay and the cone was set to be 0.2. In the calculations, samples of the different undrained shear strengths were initiated by varying of the water content only, keeping all the other model parameters constant.

Figure 5 presents the results of the investigation of the grid density influence on numerical errors. In the simulations, the number of particles remain constant at nine particles per cell. Four grid densities were taken into account which corresponds to the total material points for the kaolin clay of 600, 2400, 9600 and 23500 respectively. Figure 5 confirms that the denser grid we have, the more accurate the simulations are, as well as show the convergence of the numerical results to the theoretical solutions. For the low undrained shear strength (s_u < 3kPa), the numerical solutions converge to the theoretical solutions more rapidly than for the higher undrained shear strength (s_u >3kPa). Figure 5 also indicates that the errors for low undrained shear strength or high penetration depth simulations are lower while the errors for the high undrained shear strength or low penetration depth simulations are extremely large at the coarse grid density. As such, the accuracy convergence is faster for the deep penetration than for the low penetration.

Results shown in Figure 5 also seem to confirm that the Mohr Coulomb constitutive model with a zero friction angle (Tresca Model) extended with the strain rate dependency of cohesion and shear modulus appears to be very well suited for prediction of undrained behaviour of soft remoulded clays.

5. Validation of time dependent simulations

The validation of the fall-cone experiment was carried out with the assumption that the cone was rough and the kaolin clay in the experiment had the same characteristics as the kaolin clay in the published data [13].

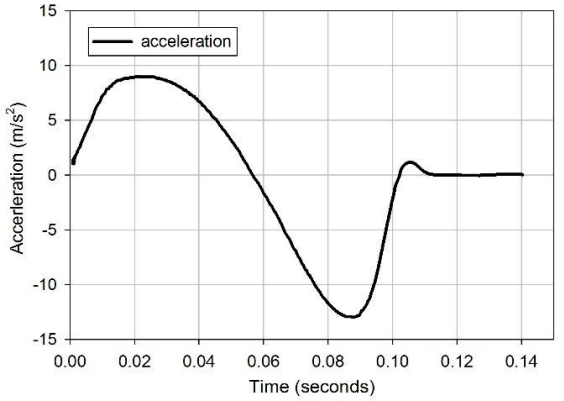

Fig. 6. Acceleration measurement during the penetration [7].

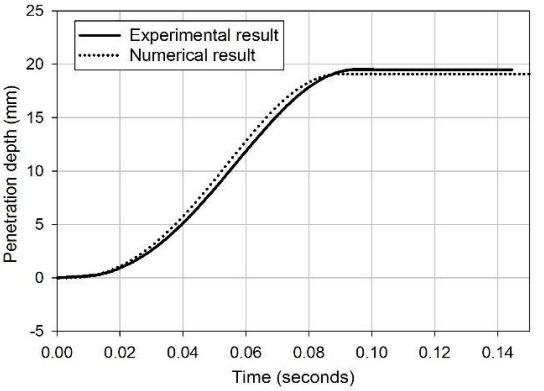

Fig. 7. Validation of the penetration depth vs. time.

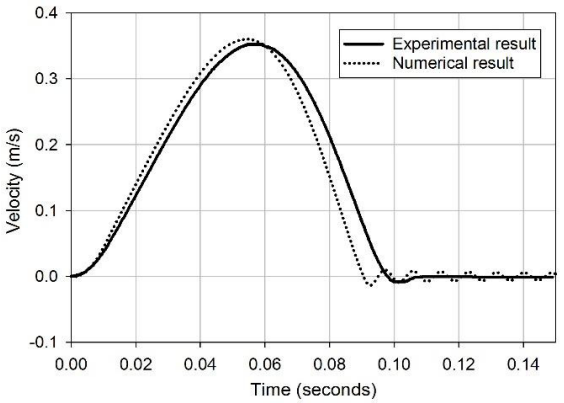

Fig. 8. Validation of the penetration velocity vs. time.

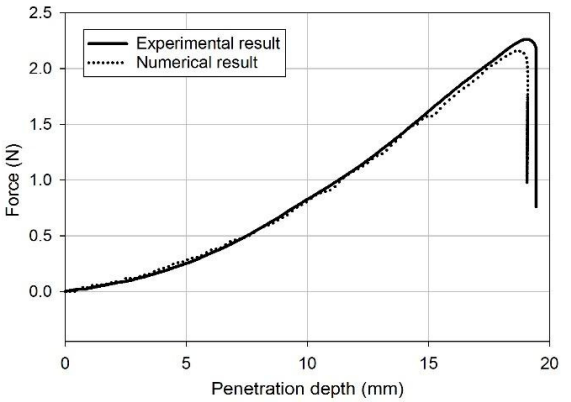

Fig. 9. Validation of the fall-cone force applying to the kaolin clay.

According to the experimental results [7], the acceleration in the beginning was less than the gravitational acceleration as in Figure 6. It means that the cone was held back during approximately 0.01s. The reason could be the friction mobilized in the cone shaft as well as the influence of equipment when releasing the cone for free-fall. This resistance became insignificant after 0.01s. In the numerical model, the resistance was modelled by a force acting in the opposite direction of the cone movement. The force was assumed to be 1N at t = 0s and it reduced gradually to zero at t = 0.01s and from that time the gravity was the only driver of the penetration process. The axi-symmetric problem dimensions are presented in Figure 4. Based on the study of the numerical errors in Section 4, the grid density was set to 0.16x0.16 mm^2 with 9 particles per cell (leading to 23,500 material points for kaolin) as it seems accurate enough for the low undrained shear strength, whereas higher grid density would lead to excessive time of computations. The kaolin clay parameters used are given in Table 1 and are the same as in the simulations where the numerical errors were investigated (Figure 5). In the calculations, the water content was selected such that it correlates to the theoretical undrained shear strength $s_{u,theo}$ = 2.7kPa. That undrained shear strength value is computed from equation 11 based on the measured penetration depth of 19.5mm.

Figure 7 compares the development of penetration depth in time in experiment and simulation. After approximately 0.1s, the cone reached the final penetration depth. The final penetration depth in the numerical model (19.1mm) is very close to the experiment (19.5mm). Furthermore, based on the study on grid density (Figure 5) it is

expected that the final penetration depth in the simulation would be even closer to the experiment if the grid density was denser.

Similarly, Figure 8 presents the velocity evolution in time. Both the numerical and experiment models predict the maximum velocity approximately at 0.35m/s after 0.06s. Finally, Figure 9 shows the force measurement of the free-fall cone in experiment and in simulation, which are, again, in very good agreement. Overall, the numerical results in terms of the evolvement of the displacement, velocity and forces in time have an excellent agreement with the experiment results.

6. Conclusions

The fall-cone test is a simple laboratory experiment to determine the undrained shear strength. The undrained shear strength interpretation depends on the angle of the fall-cone, the roughness of the cone and the strain rate parameters during the penetration. In this numerical analysis, the numerical models with the Generalized Interpolation Material Point Method combined with the Mohr-Coulomb model extended with strain-rate effects show very good agreements with both theoretical and experimental results. The penetration depths for the wide range of the theoretical undrained shear strengths and water contents are very well replicated in GIMP simulations. The experimental results [7] are very well replicated by a simulation, with excellent agreement not only of the final depth of the penetration but also the velocity and forces. The results indicate that with appropriate strain rate parameters and high grid density, GIMP simulations can successfully replicate the kinetic motion of the penetrometer. The study also suggests that the influence of strain rate effects is significant and affects greatly the kinematic behaviour of the fall-cone.

In the future, it could be interesting to investigate the capability of fall-cone in determining the strain rate parameters. With the validated numerical tools, the forces are measured could result in the bearing capacity of fall-cone under the strain rate effects.

Acknowledgements

The work has been funded by the Academy of Finland under the project ‘Progressive failure and post-failure modelling of slopes with Generalized Interpolation Material Point Method (GIMP)’, decision number is 286628.

References

[1] Nazem M, Carter JP, Airey DW, Chow SH. Dynamic analysis of a smooth penetrometer free-falling into uniform clay. *Geotechnique* 2012; 62(10):893-905.

[2] Moavenian MH, Nazem M, Carter JP, Randolph MF. Numerical analysis of penetrometers free-falling into soil with shear strength increasing linearly with depth. *Computers and Geotechnics* 2016; 72:57-66.

[3] Brannon R. Some recent advances in the Material Point Method for high-rate large-deformation penetration and blast loading. MMEC Distinguished Seminar Series, Massachusetts Institute of Technology, Cambridge, MA, 2013.

[4] Solowski W and Sloan S. Evaluation of material point method for use in geotechnics. *International Journal for Numerical and Analytical Methods in Geomechanics* 2014; 39(7):685-701.

[5] Phuong NTV, van Tol AF, Elkadi ASK, Rohe A. Numerical investigation of pile installtion effects in sand using material point method. *Computers and Geotechnics* 2016; 73:58-71.

[6] Ceccato F, Beuth L, Vermeer PA, Simonini P. Two-phase Material Point Method applied to the study of cone penetration. *Computer and Geotechnics* 2016, p. Article in press.

[7] Hazell E. Numerical and Experimental studies of shallow cone penetration in clay. Thesis at the University of Oxford, UK, 2008.

[8] Badenhagen SG, Kober EM. The generalized interpolation material point method. *Comput Model in Eng Sci* 2004; 5:477-495.

[9] Sulsky D, Zhou SJ, Schreyer HL. Application of a particle-in-cell method to solid mechanics. *Comput. Phys. Commun.* 1995; 87:236-252.

[10] Wallstedt PC, Guilkey JE. An evaluation of explicit time integration schemes for use with the generalized interpolation material point method. *Journal of Computational Physics* 2008; 227:9628-9642.

[11] Sadeghirad A, Brannon RM, Burghardt J. A convected particle domain interpolation technique to extend applicability of the material point method for problems involving massive deformations. *International Journal for numerical methods in Engineering* 2011; 86:1435-1456.

[12] Einav I, Randolph MF. Effect of strain rate on mobilized strength and thickness of curved shear bands. *Geotechnique* 2006; 56(7):501-504.

[13] Boukpeti N, White DJ, Randolph MF, Low HE. Strength of fined-grained soils at the solid-fluid transition. *Geotechnique* 2012; 62(3):213-

226.

[14] Bardenhagen SG, Brackbill JU & Sulsky D. The material-point method for granular materials. *Computational Methods in Applied Mechanics and Engineering* 2000; 187(3-4):529-541.

[15] Nairn JA and Guilkey E. Axisymmetric form of the generalized interpolation material point method. *International for numerical methods in engineering* 2015; 101: 127-147.

[16] Koumoto T and Houlsby GT. Theory and practice of the fall-cone test. *Geotechnique* 2001; 51(8):701-712.

[17] Sadeghirad A, Brannon RM, Guilkey JE. Second-order convected particle domain interpolation (CPDI2) with enrichment for weak discontinuities at material interfaces. *International Journal for numerical methods in Engineering* 2013; 95(11):928-952.

[18] Jeong SW, Leroueil S & Locat L. Applicability of power law for describing the rheology of soils of different origins and characteristics. *Canadian Geotechnical Journal* 2009; 46(9):1011-1023.